Fluids and Barriers of the CNS

RESEARCH

Open Access

Proteome profile differences among human, monkey, and mouse brain microvessels and cultured brain microvascular endothelial cells

Haruka Kumabe[1], Takeshi Masuda[1,2,3], Shingo Ito[1,2], Tomomi Furihata[4], Akiko Toda[5], Masayuki Mogi[5], Norie Araki[6] and Sumio Ohtsuki[1,2*]

Abstract

Background The blood-brain barrier (BBB) expresses transporters, receptors, and tight junction proteins that regulate the exchange of substances between the blood and brain. The differences in the expression of these proteins in the BBB among different species and cultured BBB model cells should be clarified to interpret the BBB function in model animals and cells. This study aimed to elucidate species differences among humans, monkeys, and mice and in vitro–in vivo differences in the BBB proteome using deep proteomic analysis.

Methods Brain microvessels (BMVs) were isolated from frozen cerebral cortices of human and monkey and frozen mouse cerebrums. BMVs and cultured brain microvascular endothelial cells (BMECs), such as hCMEC/D3, HBMEC/ciβ, and primary BMECs, were analyzed via data-independent acquisition using liquid chromatography-mass spectrometry.

Results Proteomics identified 7,149–8,274 proteins in the BMV fractions and 6,657–7,534 proteins in the brain lysates. Comparative analysis revealed distinct proteomic profiles among the three species, with the human profile being more similar to that of monkeys than that of mice. The expression profile of the solute carrier organic anion transporter family was found to vary among mouse, monkey, and human BMVs. The expression levels of SLC22A6/Slc22a6 and SLC22A8/Slc22a8 were higher in mice than in monkeys and humans, whereas SLC43A3/Slc43a3 expression levels were lower in mice. The expression of amino acid transporters, such as SLC7A5 and SLC3A2/Slc3a2, was higher in BMVs, whereas that of SLC1A5/Slc1a5 and SLC38A9/Slc38a9 was higher in cultured BMECs. MFSD2A/Mfsd2a and SLC27A1/Slc27a1 were highly expressed in BMVs. The expression of tight junction proteins, particularly the claudin family, varied between BMVs and cultured BMECs and among cell lines. Specifically, the expression of claudin-5 was higher in BMVs, and claudin-11 expression was higher in cultured BMECs.

Conclusions Deep proteomic analysis revealed species-specific differences in transport-related proteins in the BBB. Furthermore, in vitro and in vivo differences were observed in the transporter and claudin protein expression. This

*Correspondence:
Sumio Ohtsuki
sohtsuki@kumamoto-u.ac.jp

Full list of author information is available at the end of the article

study provides a BBB proteome profile dataset and offers insights for a comprehensive understanding of BBB protein expression across species and between in vivo and in vitro conditions.

Keywords Brain microvessels, Proteomics, Mouse, Monkey, Human, Species differences, Transporter, Cultured microvascular endothelial cells

Background

The blood-brain barrier (BBB) plays a crucial role in maintaining brain homeostasis and is composed of microvascular endothelial cells (BMECs), pericytes, and astrocytes [1]. BMECs form tight junctions with proteins such as claudin-5 and occludin, which prevent molecules in the circulating blood from entering the brain via intercellular diffusion [2]. Additionally, BMECs express various transporters and receptors responsible for the uptake of necessary molecules, such as nutrients, from the circulating blood and supply these substances to the brain parenchyma [3]. Efflux transporters are expressed in BMECs and are involved in excluding unnecessary and toxic substances from the brain parenchyma by pumping them out of BMECs into the circulating blood [1, 4]. Tight junctions and transporters in the BBB regulate drug distribution in the brain [5]. Tight junctions and ATP-binding cassette (ABC) efflux transporters limit drug distribution to the brain [6]. In contrast, solute carrier (SLC) influx transporters facilitate drug distribution in the brain by enhancing BBB permeability [7]. Therefore, the BBB plays an important role in maintaining homeostasis and drug distribution in the brain.

Previous studies have reported species differences in the BBB, which have profound implications for interpreting its function [8–10]. Our previous study has reported that ABCB1/Abcb1a (MDR1/Mdr1a), a major ABC drug efflux transporter in the BBB, is expressed at higher levels in the brain microvessels (BMVs) of mice and rats than in humans [8, 9]. A positron emission tomography comparison of the pharmacokinetics of isotopically labeled ABCB1/Abcb1a substrates in the brain showed different distributions in humans, monkeys, rats, and pigs, with reduced brain concentrations of the substrate in rats than in humans [11]. The expression of the organic anion transporter SLC22A8/Slc22a8 (OAT3/Oat3) is below the limit of quantification in human BMVs, whereas it has been detected in mice and rats [8, 9]. In contrast, ABCA8/Abca8a was not detected in the BMVs of mice or marmosets but was detected in human BMVs [8, 9]. The in vivo-in vitro differences in BBB protein expression have also been reported [12, 13]. Protein expression levels in hCMEC/D3 cells, a human BBB model cell line, were compared with those in isolated human BMVs [12]. High expression of ABCC1 (MRP1) and SLC29A1 (ENT1) was observed in hCMEC/D3 cells, whereas SLC7A5 (LAT1) was specifically expressed in human BMVs. The expression of claudin-5, a major BBB tight junction protein, decreased in hCMEC/D3 cells. Information about these differences is crucial for interpreting BBB function and brain drug distribution in humans based on the results of animal and in vitro studies.

Proteomic analysis is a useful method for characterizing the BBB through protein expression profiling. Quantitative absolute targeted proteomics (QTAP) measures the molar amounts of target proteins. We used this method to evaluate species and in vitro–in vivo differences in protein expression in BMVs [8, 12]. QTAP, instead of standard untargeted proteomics, is necessary for detecting transporters, receptors, and tight junctions with high sensitivity and quantitative accuracy. Recently, data-independent acquisition (DIA) has been developed, which provides an in-depth proteomic analysis alongside improvements in mass spectrometry [14]. Additionally, a new data analysis tool improves the identification performance, quantitative accuracy, and precision of proteomic data [15]. Multiple reports have shown that nearly 10,000 proteins can be quantified through single-shot analysis using the latest methods and instruments [16, 17]. Therefore, obtaining an in-depth proteome profiling dataset of the BBB can now be conducted to clarify novel species and in vitro–in vivo differences. These data provide a valuable reference dataset for BBB studies.

This study aimed to acquire deep protein expression profiles of BMVs isolated from frozen human, monkey, and mouse brain samples, as well as those of cultured cells used as BBB models, including several immortalized cell lines and primary cultured cells. By comparing the obtained proteomic profiles, we also clarified the species differences and differences between the in vivo and in vitro models, focusing on membrane transporters, receptors, and tight junction proteins.

Methods

Brain samples

Nine-week-old C57BL/6 N male mice were purchased from Japan CLEA (Tokyo, Japan). All mice were bred in the Kumamoto University Faculty of Pharmaceutical Sciences Animal House and housed in a 12-h light/dark environment. Mice were dissected at 10 weeks of age, and the cerebrum was collected after perfusion with 1× phosphate-buffered saline (PBS) from the heart for 5 min at a flow speed of 17.5 mL/min. Frozen cerebral cortices from cynomolgus monkeys without perfusion were obtained from Shin Nippon Biomedical Laboratories (Kagoshima, Japan). A cynomolgus monkey's cerebral cortices were

collected after anesthesia with intramuscular administration of ketamine hydrochloride (50 mg/mL, 0.1–0.3 mL/kg) and medetomidine hydrochloride (1 mg/mL, 0.08 mL/kg) and exsanguination through transection of the axillary and femoral arteries and veins. Frozen human cerebral cortices without perfusion were purchased from ProteoGenex (Inglewood, CA, USA). Human brain samples were obtained following official protocols with appropriate Institutional Review Board/Independent Ethics Committee approval, which adhered to current Federal Regulations, the International Council for Harmonization of Technical Requirements for Pharmaceuticals for Human Use, Health Insurance Portability and Accountability Act of 1996, and Guideline for Good Clinical Practice guidelines for the protection of human subjects. The conditions for the monkey and human cerebral cortex samples are listed in Table S1. All animal experiments were approved by the Institutional Animal Care and Use Committee at Kumamoto University (approval no. A2021-041 and A2023-046) and Shin Nippon Biomedical Laboratories (approval no. IACUC20241220-1-50), following the Fundamental Guidelines for Proper Conduct of Animal Experiments and Related Activities in Academic Research Institutions under the jurisdiction of the Ministry of Education, Culture, Sports, Science, and Technology of Japan and in accordance with the Animal Research: Reporting in Vivo Experiment Guidelines.

Isolation of microvessels from frozen brain

BMVs were isolated from frozen human and monkey cerebral cortices and frozen mouse cerebrum, as previously described [18, 19]. Briefly, a single frozen mouse brain was homogenized in 1 mL of homogenization buffer (101 mM NaCl, 4.6 mM KCl, 2.5 mM $CaCl_2$, 1.2 mM KH_2PO_4, 1.2 mM $MgSO_4$, and 15 mM (4-(2-hydroxyethyl)-1-piperazineethanesulfonic acid), pH 7.4) using a bead homogenizer (Bead Mill 4, Thermo Fisher Scientific, Waltham, MA, USA) for 60 s at 3 m/s with stainless steel beads (3.2 mm, 1.8 g; TOMY SEIKO, Tokyo, Japan). Fifty microliters of the brain homogenate was collected in another tube as the brain lysate. The homogenate was centrifuged (4500 × g, 10 min, 4 °C), and the supernatant was removed. The pellet was suspended in 1 mL of homogenization buffer, and 1 mL of 32% (w/v) dextran/homogenization buffer was added. After mixing by inverting, the samples were immediately centrifuged (4500 × *g*, 15 min, 4 °C). The supernatant was collected in another tube and centrifuged (4500 × *g*, 15 min, 4 °C) once again. The pellet was suspended in 400 µL of suspension buffer (homogenization buffer containing 25 mM $NaHCO_3$, 10 mM glucose, 1.2 mM pyruvate, and 5 g/L bovine serum albumin) and filtered through a cell strainer (70 µm). Glass beads were added to a new cell strainer and washed four times with 500 µL of suspension buffer. The suspension was added to the strainer and washed 10 times with 500 µL of suspension buffer. The glass beads were collected in a 2 mL tube, and suspension buffer was added. After centrifugation (3300 × *g*, 5 min, 4 °C), the supernatant was removed, and the samples were suspended in 200 µL of homogenization buffer. A portion of the BMV fraction was used for microscopy, and the remaining BMV sample was lysed in a phase transfer surfactant buffer (PTS buffer: 12 mM sodium deoxycholate, 12 mM N-lauroylsarcosinate, and 50 mM triethylammonium bicarbonate) through sonication [20]. Protein concentration was measured using a Pierce bicinchoninic acid protein assay kit (Thermo Fisher Scientific). Human and monkey BMVs were isolated from 0.6 to 0.8 g of frozen brain blocks. Brain blocks were cut in half, and BMVs were isolated using the same method as for mouse brains. After isolation, two BMV samples from the same brain block were combined and lysed in the PTS buffer.

Cell culture

MBEC4 cells, immortalized mouse brain microvascular endothelial cells, were cultured in Dulbecco's modified Eagle medium supplemented with 10% fetal bovine serum (Biowest, Nuaille, France) and 1% penicillin–streptomycin [21]. As immortalized human brain microvascular cells, hCMEC/D3 and HBMEC/ciβ cells were cultured in Endothelial Cell Growth Basal Medium-2 (Lonza, Basel, Switzerland) supplemented with 5% fetal bovine serum, 1% penicillin–streptomycin, 1% chemically defined lipid concentrate, 10 mM (4-(2-hydroxyethyl)-1-piperazineethanesulfonic acid), 1.4 µM hydrocortisone, 1 ng/mL of human basic fibroblast growth factor, 5 µg/mL ascorbic acid, and 424 µg/mL LiCl in an atmosphere of 95% air and 5% CO_2 at 37 °C or 33 °C for hCMEC/D3 or HBMEC/ciβ, respectively [22, 23]. After the HBMEC/ciβ cells became confluent, the temperature was changed to 37 °C for an additional three days for differentiation [24]. Primary human brain microvascular endothelial cells (prBMECs) were obtained from KAC Corporation (Kyoto, Japan) and cultured using the CS-C Complete Medium Kit R (KAC Corporation, Kyoto, Japan). Human umbilical vein endothelial cells (HUVECs) were obtained from Promocell (Heidelberg, Germany) and cultured in an endothelial cell growth medium (Promocell). prBMEC and HUVECs were cultured in an atmosphere of 95% air and 5% CO_2 at 37 °C. All cells were seeded at $0.5–1.0 \times 10^5$ cells onto collagen-1 coated 100 mm dishes (Corning, Glendale, AZ, USA) for 3–5 days to reach confluence.

Cell sample preparation for proteomic analysis

Confluent cells were collected using scrapers, washed with 1× PBS, and centrifuged (1000 × *g*, 4 °C, 5 min). After centrifugation, the supernatant was removed, and

the pellet was suspended in PTS buffer. For targeted proteomic analysis, the crude membrane was fractionated from MBEC4 and hCMEC/D3 cells [25]. Four dishes of confluent cells were washed three times with 1× PBS, collected in a 15-mL tube with scrapers, and centrifuged (4500 × *g*, 4 °C, 5 min). After centrifugation, the supernatant was removed, and the pellet was suspended in 500 µL of homogenized buffer containing a protein inhibitor cocktail. Cells were lysed using a Dounce homogenizer on ice, and the debris was removed through centrifugation (700 × *g*, 4 °C, 10 min). The supernatant was collected as the cell lysate in a 1.5-mL tube, and the debris was removed again. The supernatant was collected and centrifuged (10000 × *g*, 4 °C, 30 min). The pellet was collected as a crude membrane and resuspended in the PTS buffer. All cell lysates and crude membrane samples were solubilized through sonication, and the protein concentration was measured using a bicinchoninic acid protein assay kit (Thermo Fisher Scientific).

Western blot analysis

Brain lysates and the isolated BMV fractions were treated with sodium dodecyl sulfate sample buffer containing 50 mM dithiothreitol. Proteins were separated on 8% sodium dodecyl sulfate-polyacrylamide gels and blotted onto polyvinylidene difluoride membranes (Thermo Fisher Scientific). The membranes were blocked with 3% skimmed milk in Tris-base buffer containing 0.1% polyoxyethylene(20) sorbitan monolaurate, and then immunoblotted with the following primary antibodies: anti-claudin-5, 1/1500, overnight at 4 °C (35–2500; Thermo Fisher Scientific), anti-PSD95/Psd95, 1/1500, overnight at 4 °C (2507S; Cell Signaling Technology, Danvers, MA, USA), and HRP-conjugated anti-β-actin, 1/2500, for 1 h at room temperature (12262S; Cell Signaling Technology). The blots were incubated with HRP-conjugated secondary antibody (7076S or 7074S; Cell Signaling Technology), and imaged with Western BLoT Hyper HRP Substrate (Takara Bio Inc., Shiga, Japan) using an Omega Lum G imaging system (Gel Company, Inc., San Francisco, CA, USA) and an iBright imaging system (Thermo Fisher Scientific).

Quantitative proteomic analysis

Protein samples were digested with trypsin using the PTS method, as previously described [20]. Peptide samples from mice, humans, and cultured cells were analyzed using DIA with an Orbitrap Fusion Tribrid coupled with an Easy-nLC 1200 (Thermo Fisher Scientific). The mass spectrometry parameters were established based on published data [26], with a 2 h gradient, variable window, and StepCE (22, 24, 26) of higher-energy collisional dissociation collision energy. One microgram of each peptide was separated using a C18 column and injected into a mass spectrometer. Raw measurement data were converted into mzML files using msConvert (https://proteowizard.sourceforge.io/projects.html). Monkey brain, BMV, and mouse BMV samples were analyzed using a Dionex Ultimate 3000 RSLCnano System (Thermo Fisher Scientific) coupled with a ZenoTOF 7600 mass spectrometer (SCIEX, Framingham, MA, USA). Two to three hundred nanograms of each peptide were separated using a C18 column with a 70 min gradient, as previously described [16, 27].

Proteins were identified and quantified using the library-free search function in the DIA-NN 1.8.1. The data were analyzed using the MaxLFQ algorithm incorporated into the DIA-NN [28]. The precursor FDR was set at 1%. Reference proteome FASTA files with one protein sequence per gene were downloaded from the UniProt proteome database (https://www.uniprot.org/proteomes; UP000005640 for humans; UP000233100 for cyno molgus monkeys; and UP000000589 for mice). Monkey samples were analyzed using human proteome FASTA files because there was no database containing sufficient information. The quantitative values from ZenoTOF 7600 were normalized to those from fusion using the following equation, determined from the values of the same mouse BMV samples:

$$Q_F = 10^{\{(\log_{10} Q_z + 0.4693)/0.8208\}}$$

where Q_F and Q_Z are the protein expression values obtained using Fusion and ZenoTOF7600, respectively. Protein intensities were normalized by dividing by the total intensity of all molecules in each sample (Table S2, S3, and S4), and the distribution diagram of the protein expression profiles is shown in Fig. S1A. Among the quantified proteins, molecules with at least one transmembrane region and Gene Ontology (GO) terms of "Transporter activity" were extracted as transporters, and molecules with GO terms of "Signal transduction" were extracted as receptors. For ortholog analysis, mouse and human gene information was obtained from the National Center for Biotechnology Information (https://www.ncbi.nlm.nih.gov/), and the protein database was obtained from UniProt (https://www.uniprot.org/). Mouse gene information was converted into the corresponding human genes using Alliance of Genome Resources (http://alliancegenome.org/downloads) as orthologous molecules (database version 8.0.0). Pseudogenes were removed from the list of orthologs. The quantitative values of each molecule are annotated in the corresponding table (Table S5), and species differences were analyzed. Raw data files for liquid chromatography-linked mass spectrometry analysis have been deposited in jPOST (http://jpostdb.org, jPOST ID: JPST003553/PXD06008).

Quantitative targeted absolute proteomics for SLC43A3/Slc43a3

The amount of SLC43A3/Slc43a3 (ENBT1/Enbt1) in the crude membrane fractions of MBEC4 and hCMEC/D3 was determined using QTAP with multiple reaction monitoring analysis, as previously described [29]. Briefly, proteins in the crude membrane fraction were digested with trypsin using the PTS method as previously described [20], and stable isotope-labeled peptides (Cosmo Bio, Tokyo, Japan) were added to the digested peptide as an internal standard. The PTS buffer was removed, and the samples were desalted. The peptide samples were analyzed using a ZenoTOF 7600 mass spectrometer interfaced with a Dionex Ultimate 3000 RSLCnano System. The standard peptide sequences used were GHIPYPPNYGLCSR for mouse Slc43a3 and SFWSYAFSR for human SLC43A3. The R at the C-terminus was substituted with R ($^{13}C_6$, $^{15}N_4$) in the internal standard peptides. The transitions (Q1/Q3) for mouse Slc43a3 peptides are 697.7/195.09+, 697.7/308.17+, 697.7/568.29+, 697.7/778.42+, and 697.7/1216.54 + for the standard peptide and 701.0/195.09+, 701.0/308.17+, 701.0/568.29+, 701.0/778.42+, and 701.0/1226.55 + for the internal standard peptide. Those for human SLC43A3 peptides are 575.8/235.11+, 575.8/480.26+, 575.8/643.32+, 575.8/730.35+, and 575.8/916.43 + for the standard peptide and 580.8/235.11+, 580.8/490.26+, 580.8/653.33+, 580.8/740.36+, and 580.8/926.44 + for the internal standard peptide. Multiple reaction monitoring data were analyzed using Skyline 23.1 (MacCoss Laboratory, University of Washington, WA, USA). SLC43A3/Slc43a3 expression levels were determined from the average values of the peak area ratios of the five sets of transitions.

RNA sequencing

Each cell pellet was collected in the same manner as for proteomic analysis. Total RNA was extracted from the cell pellets using an RNA extraction kit (Qiagen, Venlo, Netherlands). RNA sequencing was performed by Macrogen (Seoul, Korea), and mRNA concentration was quantified. Data were analyzed using Galaxy Version 23.2.1. (https://usegalaxy.org/). Data on read counts and transcript lengths for each molecule were obtained, and transcripts per million (TPMs) were calculated. To ensure data reliability, molecules with TPM > 1 were selected for analysis. Each TPM of the gene was normalized by dividing it by the total intensity of all molecules in each sample (Fig. S1B).

Statistical analysis

Numerical data are expressed as the mean ± standard deviation (SD). The statistical significance of the differences between two groups was determined using a two-tailed Student's t-test in Microsoft Excel (Microsoft, Redmond, WA, USA). Multiple groups were compared using one-way ANOVA followed by Tukey's post-hoc test with GraphPad Prism7 (GraphPad, Boston, MA, USA). For testing multiple molecules, *p*-values were adjusted using the Benjamini-Hochberg method, referred to as the adjusted *p*-value. Principal component and cluster analyses were conducted using SIMCA14 software (Sartorius, Göttingen, Germany). GO enrichment analysis was performed using DAVID 2011 referring to all identified orthologous proteins as background (https://david.ncifcrf.gov/), and graphs were created using GraphPad PRISM9.

Results

Isolation of microvessels from mouse, monkey, and human brain

We isolated BMVs from the frozen cerebrums of mice (C57BL/6N) and frozen cerebral cortices of cynomolgus monkeys and humans using previously reported methods [18, 19]. Microscopic images showed that BMVs were isolated from all the sample types (Fig. 1A). Western blotting was performed to evaluate BMV enrichment in the isolated fractions (Fig. 1B). Claudin-5, which is specifically expressed in BMECs, was clearly detected in the BMV fractions of all species but was barely detectable in brain lysates (Fig. 1B top panels). PSD95/Psd95, a neuronal marker, was detected in the brain lysates of all species but not in the BMV fractions (Fig. 1B, middle panels). These results suggested that BMVs were enriched in the isolated fractions, indicating that proteomic analysis could be conducted with similar enrichment among biological replicates of all species.

Proteomic analysis of isolated brain microvessels

BMVs isolated from mouse, monkey, and human brain were analyzed using DIA proteomics, as described in Materials and Methods. The proteins were identified using the UniProt reference proteome database. However, we found incompleteness in the monkey reference proteome database because it did not contain the amino acid sequences of proteins important for BBB function, such as ABCB1, ABCG2, and claudin-5. Given that the genetic difference between human and monkey genomes is approximately 4% [30], the DIA data of monkey BMVs and the brain were analyzed using either the monkey or human reference proteome database, and the identification and quantification data of the two proteome results were compared (Fig. 2). The numbers of identified proteins in the BMV fractions and brain lysates were not significantly different between the data analyzed with monkey and human reference proteome database files (Fig. 2A). The quantified values of proteins in the BMV fractions and brain lysates (total 12,288 proteins) were significantly correlated with the monkey and human

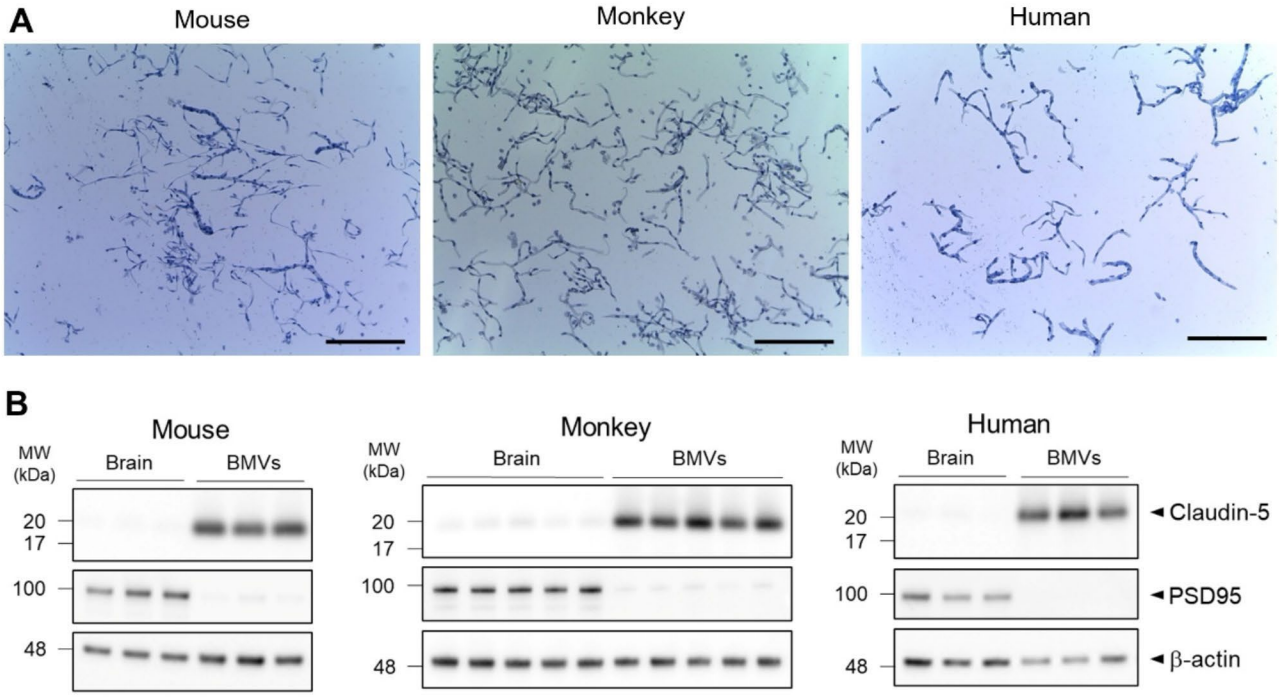

Fig. 1 Isolation of microvessels from mouse, monkey, and human brain. **A** Images of the microvessel fraction isolated from frozen mouse, monkey, and human brain. Scale bar; 250 µm. **B** Western blot analysis of claudin-5 and PSD95 in mouse, monkey, and human whole-brain lysate and the fraction of brain microvessels (BMVs) fraction. The sizes of molecular weight (MW) markers are indicated on the left side of the image

reference proteome database files ($p < 0.0001$), and 75.6% of proteins were showing a 1.5-fold difference (Fig. 2B and C). Based on these results, we used a human reference proteome database for protein identification and quantification in the monkey samples. This allowed us to quantify, on average, 7,149–8,274 proteins in the BMV fractions and 6,657–7,534 proteins in the brain lysates (Fig. 2D; expression data are shown in Table S2-S4).

Proteomic and RNA-seq analyses of cultured BMECs

We also analyzed the protein and mRNA expression in cultured BMECs using proteomic and RNA-seq analyses, respectively. The average number of identified proteins ranged from 7,676 to 8,460, and that of identified genes ranged from 10,874 to 11,527 (Fig. 3A; expression data are shown in Tables S5 and S6). In all samples, the number of identified genes was greater than the number of proteins. Over 64% of the molecules detected in RNA-seq were identified using proteomics, and conversely, over 90% of the molecules identified using proteomics were also identified using RNA-seq (Fig. 3B for immortalized cells and Fig. S2A for primary BMECs and HUVEC). These results indicate the reliability of protein identification in the present proteomic analysis. A comparison of gene and protein intensities in each sample revealed a significant but broad correlation of intensities between gene and protein ($r < 0.67$) with a median gene-to-protein intensity ratio of 1.41–2.45 fold, and the ratios varied in the range of 2.46×10^{-4} to 8.66×10^{3} (Fig. 3C for immortalized cells and Fig. S2B for primary BMECs and HUVECs).

Comparison of proteome profile in mouse, monkey, and human brain microvessels

To elucidate the species differences in proteins expressed in the BBB, we compared the protein expression levels in the BMV fractions of the three species. A human-mouse ortholog table was created based on mouse and human gene databases, as described in the Materials and Methods section, and the proteome data were annotated (Table S5). A total of 12,272 orthologous proteins were identified, and 6,845 proteins were identified in all three species (Fig. 4A).

The BMV fractions cannot fully exclude the contamination of brain cells other than BMECs, such as neurons, pericytes, and astrocytes. To exclude protein data derived from contaminated brain cells, proteins significantly enriched in the BMV fractions compared with brain lysates were selected as BMV-enriched proteins [$\log_2$ (ratio of BMVs / brain) > 2.5, adjusted p-value < 0.05]; 1,636 proteins in mice, 1,166 proteins in monkeys, and 2,155 proteins in humans (Table S5). In mice, 13 known BMEC-selective proteins were selected as BMV-enriched proteins. In monkeys and humans, 11 and nine of the 13 BMEC-selective proteins, respectively, were selected as BMV-enriched proteins (red dots, Fig. 4B). In monkeys,

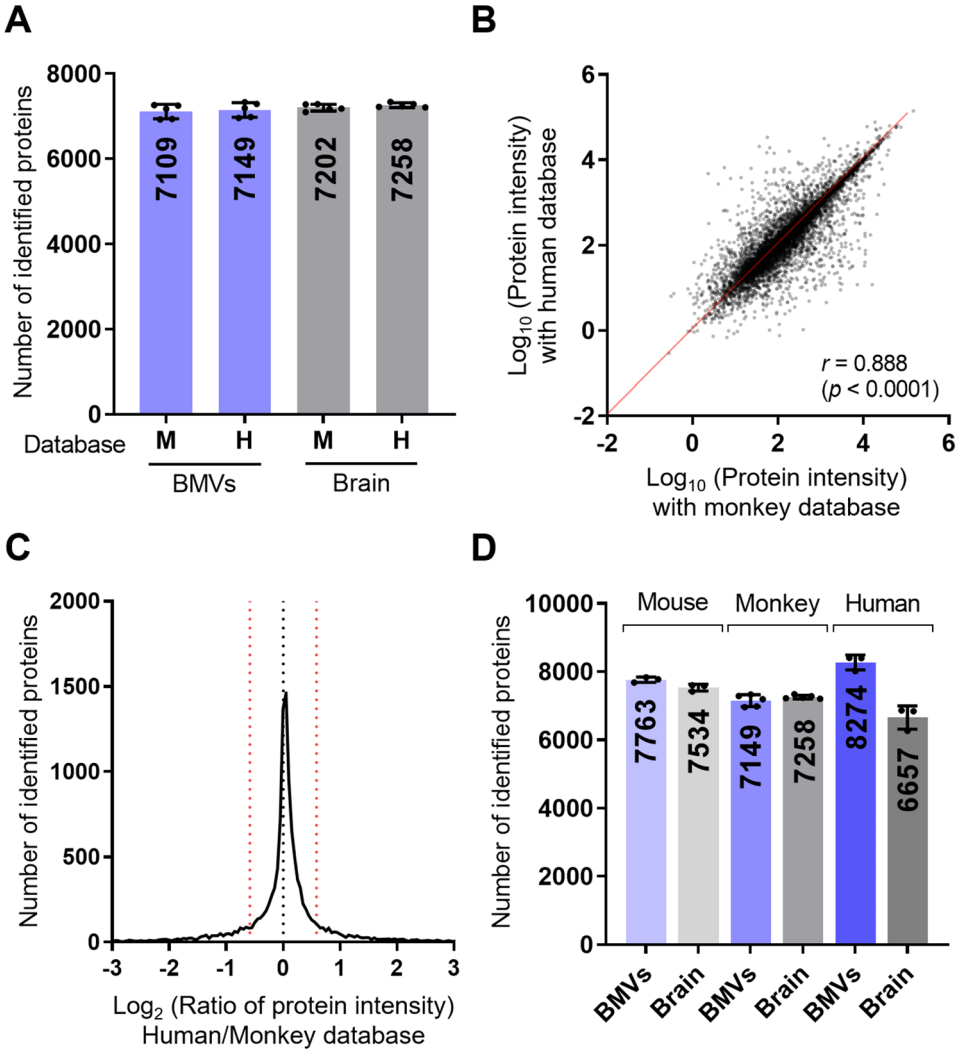

Fig. 2 Protein identifications in mouse, monkey, and human BMV fractions and brain lysates. **A** Number of proteins identified in the monkey BMV fractions and brain lysates analyzed using either monkey (M) or human (H) reference proteome databases ($n = 5$). **B** Correlation comparison of protein intensity quantified in monkey BMV fractions and brain lysates between analyses using monkey and human reference proteome databases containing a total of 12,288 proteins. The solid red line represents a ratio of 1:1. **C** Frequency distribution of the protein intensity ratio of the data quantified of monkey BMV fractions and brain lysates analyzed using monkey and human reference proteome databases containing a total of 12,288 proteins. The dashed red lines indicate the ratio of 0.667 and 1.50. **D** Number of proteins identified in BMV fractions and brain lysates of each species ($n = 3$–5). Each bar represents the mean ± SD. The numbers in the bar represent the averages, and dots indicate the individual data

one protein showed a low $\log_2$ (ratio of BMVs / brain) (light red dot, Fig. 4B). In humans, two proteins indicated low $\log_2$ (ratio of BMVs / brain) and adjusted p-values > 0.05 (light red dots, Fig. 4B). PSD95/Psd95, a neuronal marker, was not found among the BMV-enriched proteins in either species (blue dots, Fig. 4B).

The differences in the proteome profiles of proteins enriched in the BMVs of the three species (3,053 proteins, Fig. 4A) were analyzed using principal component analysis (PCA) and clustering analysis (Fig. 4C). The proteome profile of each species formed a cluster, and the human profile was closer to that of monkeys than to that of mice in the first component of the PCA and in the distance of clustering analysis.

Species differences of transport-related protein expression in brain microvessels

We compared the protein expression levels of transporters, for which we reported species differences in their expression using QTAP [8], to assess the reproducibility of the present multi-species proteome data (Fig. 5A). In a previous report, the ratios of ABCB1/Abcb1a and ABCG2/Abcg2 (BCRP/Bcrp) to mice in humans were 0.430- and 1.85-fold, respectively [8, 31]. Slc22a8 was detected only in mice, and ABCA8 was only detected in humans [8]. These species differences were reproduced in the present study, with human-to-mouse ratios of 0.344- and 1.57-fold for ABCB1/Abcb1a and ABCG2/Abcg2, respectively, and species-specific detection of SLC22A8/

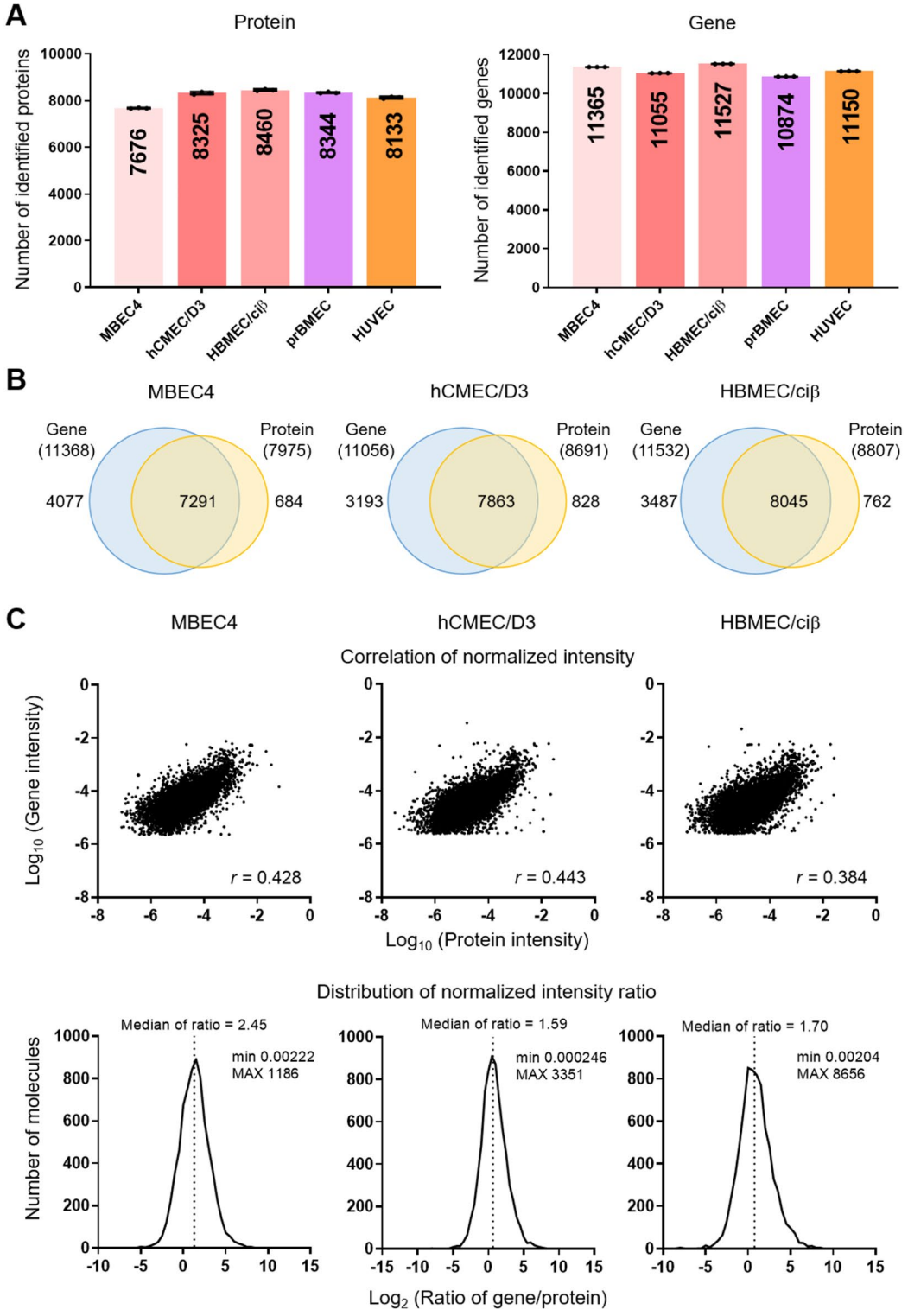

Fig. 3 Proteomic and RNA-seq analyses of cultured BMECs. **A** Number of identified proteins and genes in cultured cell samples. Each data point represents the mean ± SD ($n = 3$). The numbers in each bar represent the averages of the data, and dots indicate the individual data. **B** Ven diagrams of the identified genes and proteins for profiles obtained from hCMEC/D3, HBMEC/ciβ, and MBEC4 cells. Numbers in parentheses indicate the total identified genes or proteins. **C** Correlation of normalized intensities between genes and proteins (top), and the distribution of gene-to-protein normalized intensity ratio (bottom). The dashed lines represent the median of the ratio (MBEC4: 2.45, hCMEC/D3: 1.59, and HBMEC/ciβ: 1.70). Maximum and minimum ratios were indicated as MAX and min, respectively

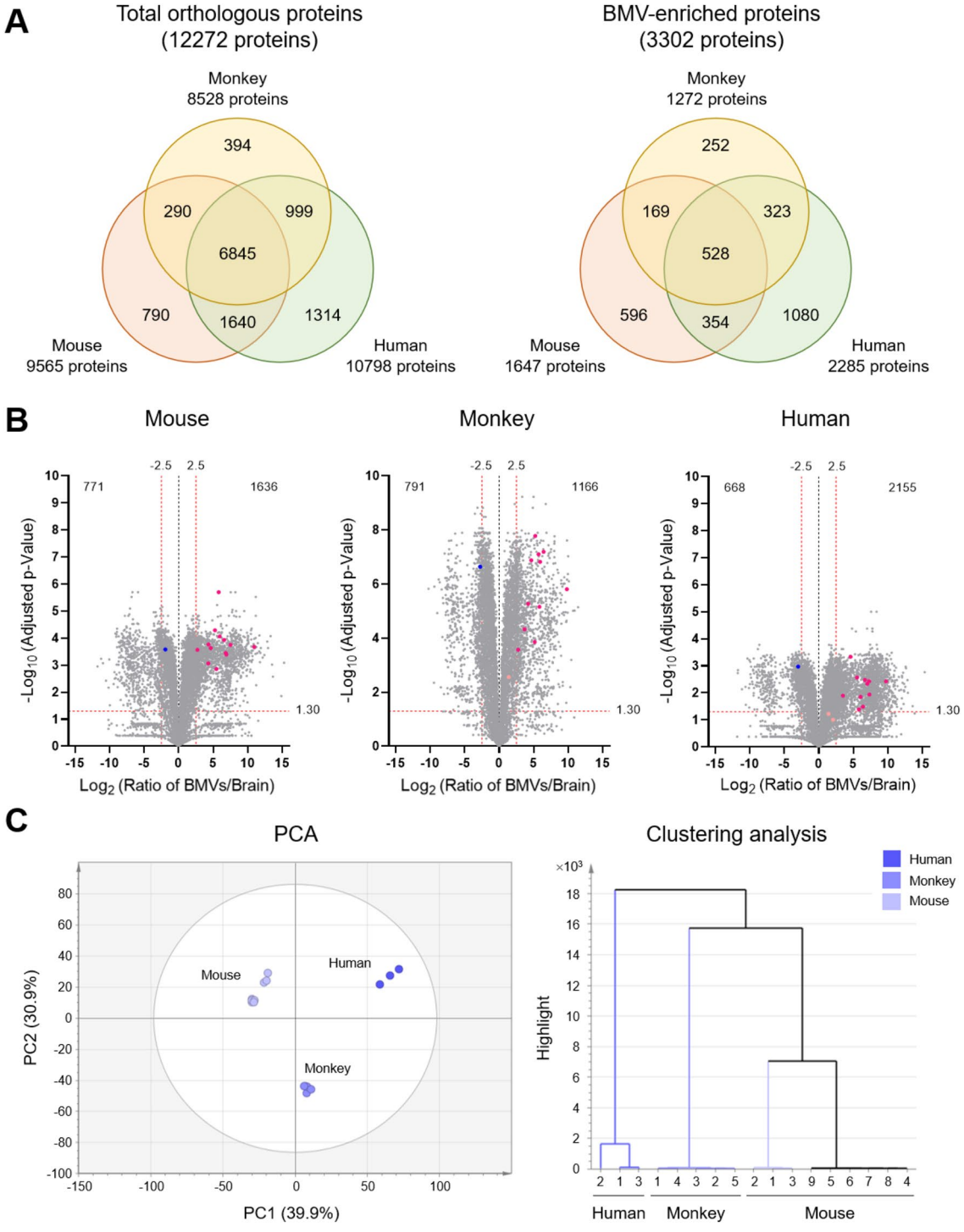

Fig. 4 Ortholog analysis of proteome profile in mouse, monkey, and human BMV fractions. **A** Overlap of orthologous proteins (left) and BMV-enriched proteins (right) identified in the BMV fractions from mice, monkeys, and humans. **B** Volcano plot of identified proteins in the BMV fractions and brain lysate in each species. The dashed red lines indicate thresholds of criteria for BMV-enriched proteins [$\log_2$ (ratio of BMVs/brain) = 2.5 and adjusted $p = 0.05$]. The red dots represent BMEC-selective proteins (ABCG2/Abcg2, ABCB1/ABcb1a, ABCC4/Abcc4, SLC22A1/Slc22a1, SLC7A5/Slc7a5, TFRC/Tfrc, INSR/Insr, CLDN5/Cldn5, OCLN/Ocln, PECAM1/Pecam1, ESAM/Esam, VWF/Vwf, and TIE2/Tie2). The BMEC-selective proteins out of the criteria for BMV-enriched proteins are indicated as light red dots. Blue dots represent neuron-selective protein (PSD95/Psd95). **C** PCA and clustering analysis of BMV-enriched protein profile in mouse, monkey, and human BMV fractions. The numbers on the samples indicate the replicate numbers of each species. The same samples of mouse BMVs were measured using different instruments (Fusion: samples 1–3, ZenoTOF 7600: samples 4–6). Replicates of BMVs isolated using the same method were also measured using the ZenoTOF 7600 (samples 7–9)

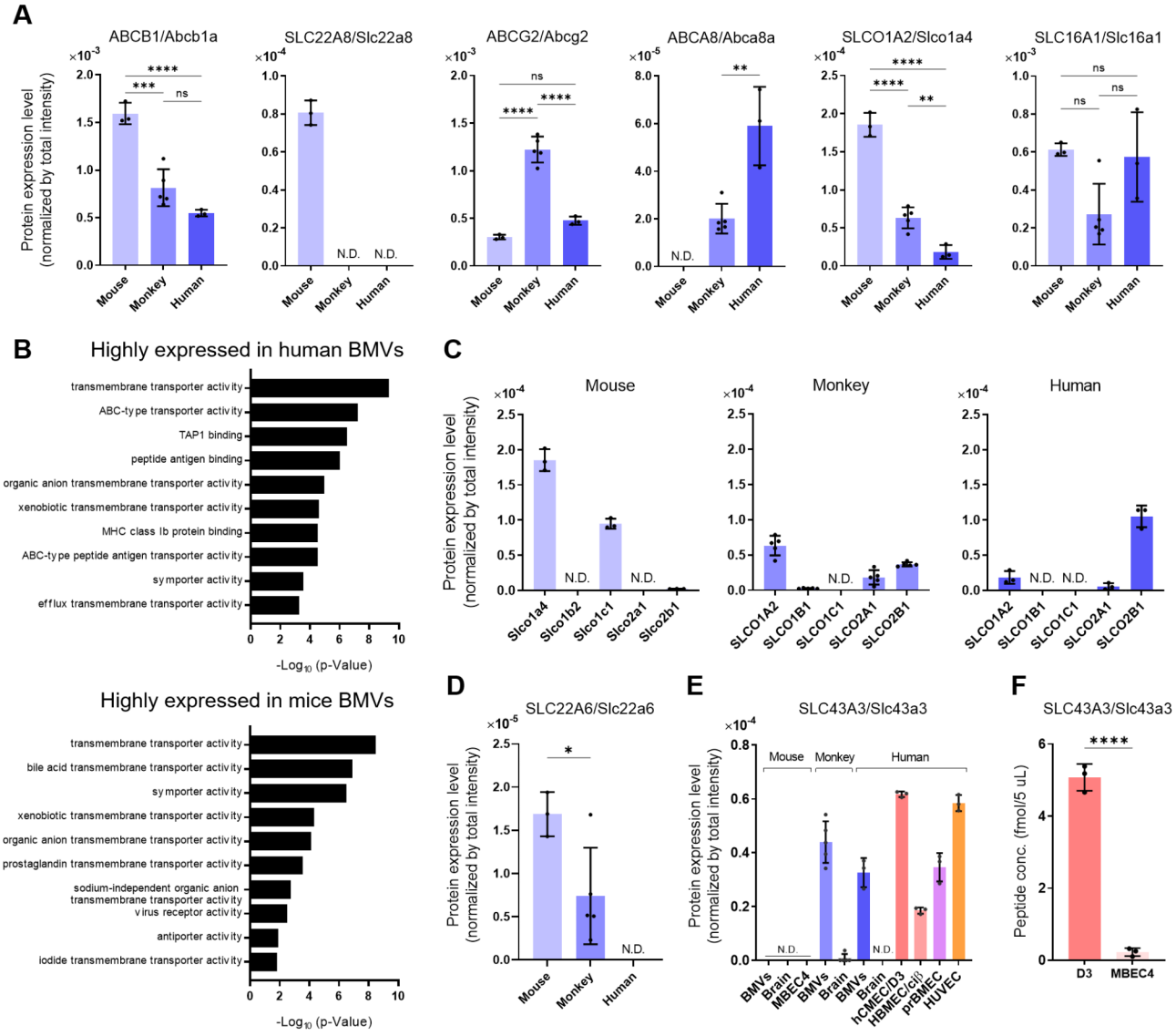

Fig. 5 Species differences in protein expression in mouse, monkey, and human BMVs. **A** Protein expression levels of blood-brain barrier transporters in mouse, monkey, and human BMVs. Statistical analyses were performed using one-way ANOVA with Tukey's test. $^{**}p < 0.01$, $^{***}p < 0.001$, and $^{****}p < 0.0001$. **B** Gene Ontology (GO) enrichment analysis of BMV-enriched proteins highly expressed in either human or mouse BMVs. The top 10 enriched GO terms or biological processes are shown. **C.** Expression levels of SLCO family proteins in mouse, monkey, and human BMVs. The corresponding orthologs are SLCO1A2/Slco1a4, SLCO1B1/Slco1b2, SLCO1C1/Slco1c1, SLCO2A1/Slco2a1, and SLCO2B1/Slco2b1. **D** SLC22A6/Slc22a6 expression levels in mouse, monkey, and human BMVs fraction. Statistical analyses were performed using one-way ANOVA with Tukey's test. $^{*}p < 0.05$. **E** SLC43A3/Slc43a3 expression level in BMV fractions and brain lysates in three species. **F** Protein expression levels of SLC43A3/Slc43a3 in the crude membranes of hCMEC/D3 and MBEC4 measured using QTAP with an internal standard peptide. Each data represents the mean ± SD ($n = 3$–5). Statistical analyses were performed using a two-tailed Student's t-test. $^{****}p < 0.0001$

Slc22a8 and ABCA8/Abca8a (Fig. 5A). The expression of these transporters in monkeys is similar to that observed in humans. However, ABCG2 expression in monkeys was 2.57-fold higher than that in humans, and the expression of ABCA8 in monkeys was 34.2% lower than that in humans. In a comparison between monkeys and humans, SLCO1A2 was previously quantified only in monkeys, whereas SLC16A1 (MCT1) was approximately 3-fold higher in humans than in monkeys [10]. In the present study, the ratios of SLCO1A2 and SLC16A1 to monkeys in humans were 0.291- and 2.10-fold, respectively (Fig. 4A). Thus, the species differences in these transporters were reproduced in this study.

Further species difference analysis focused on transport-related proteins (transporters and receptors) in BMV-enriched proteins, as transport functions play an important role in regulating the blood-brain exchange and drug distribution in the brain. In humans, 19 transport-related proteins were expressed more than 4-fold, and 16 proteins were detected only in humans (Table S7).

In contrast, 17 transport-related proteins were expressed over 4-fold higher in mice, and 27 proteins were detected only in mice (Table S8). A comparison of the expression levels of transport-related proteins between human and monkey brain capillaries revealed that 19 transport-related proteins were expressed over 4-fold higher in humans, and 29 proteins were detected only in humans (Table S9). In contrast, 10 transport-related proteins were expressed over 4-fold higher in monkeys, and eight proteins were detected only in monkeys (Table S10).

A GO enrichment analysis of transport-related proteins revealed that organic anion transport-related terms, such as "organic anion transmembrane transporter activity" and "sodium-independent organic anion transmembrane transporter activity," were enriched in humans and mice (Fig. 5B). When focusing on the organic anion transporters, we observed species differences in the SLCO family expression profiles and SLC22A6/Slc22a6 (OAT1/Oat1) (Fig. 5C and D). SLCO2B1 expression was predominantly observed in humans, and Slco1a4 and Slco1c1 were predominantly observed in mice. These transporter proteins were significantly enriched in the BMV fractions, exhibiting more than a 5-fold increase compared to brain lysates (adjusted p-value < 0.05), except for human SLCO1A2 and SLCO2A1 (Table S12). These two transporter proteins showed BMV-enrichment ratios > 5 and adjusted p-values of 0.0691 and 0.177, respectively. Therefore, SLCO/Slco proteins detected in the present study are suggested to be expressed in BMVs. SLC22A6/Slc22a6 was more highly expressed in mice than in humans or monkeys (Fig. 5D). As a molecule involved in drug transport, we focused on SLC43A3/Slc43a3, which is specifically expressed in human and monkey BMVs. (Fig. 5E). To confirm the species-specific expression of SLC43A3/Slc43a3, we performed QTAP analysis of SLC43A3/Slc43a3 using internal standards in hCMEC/D3 and MBEC4 cells. This analysis revealed that expression in hCMEC/D3 cells was 22.4-fold higher than in MBEC4 cells (Fig. 5F), confirming the protein expression results obtained from DIA proteomics (Fig. 5E).

Comparison of proteome profiles between BMVs and cultured BMECs

To investigate proteomic differences in the BBB between in vivo and in vitro conditions, we first compared the expression profiles of human BMVs and cultured human cells using PCA and clustering analysis with proteins enriched in the human BMV fraction (Fig. 6A). Primary cultured human BMECs had the closest profile to human BMVs compared with immortalized human BMECs (hCMEC/D3 and HBMEC/ciβ) and HUVECs in the first component of PCA and clustering analysis. We then assessed the reproducibility of the proteomic data by comparing them with data reported previously using QTAP [12]. In a previous comparison of hCMEC/D3 with human BMVs, ABCC1 was identified only in hCMEC/D3, and SLC29A1 (ENT1) was 11.7-fold higher in hCMEC/D3. SLC7A5 was identified only in isolated human BMVs, and claudin-5 expression was 5.27-fold higher in isolated BMVs. In the present analysis, ABCC1 and SLC29A1 were 11.3- and 1.54-fold more abundant in hCMEC/D3 cells than in isolated BMVs, respectively (Fig. 6B). In contrast, SLC7A5 expression was 5.79-fold higher in human BMVs than in hCMEC/D3. Claudin-5 was identified only in BMVs (Fig. 6B).

A GO enrichment analysis was conducted for proteins enriched in BMV and differentially expressed by over 2-fold (adjusted p-value < 0.05) in in vitro (hCMEC/D3 and MBEC4) and in vivo (BMVs) conditions in humans and mice (Table S12). As a result, 233 differentially expressed proteins enriched in BMVs were identified as proteins that were highly expressed in vitro, and GO terms related to transcription and RNA processing were enriched (Fig. 7A). Amino acid transporters not only regulate cell proliferation but also mediate amino acid transport across the BBB [32, 33]. Among these amino acid transporters, SLC1A5/Slc1a5 and SLC38A9/Slc38a9 were highly expressed in vitro (Fig. 7B). A total of 218 proteins that were highly expressed in vivo were identified, with enriched GO terms related to cell adhesion, extracellular matrix, and blood-brain barrier maintenance (Fig. 7A). Among molecules related to the transport of amino acids and docosahexaenoic acid (DHA), SLC3A2/Slc3a2 and MFSD2A/Mfsd2a were highly expressed in vivo (Fig. 7B). Although not significantly enriched in BMVs, SLC27A1/Slc27a1, a molecule that transports DHA, was quantified at higher levels in vivo than in vitro (Fig. 7B).

The claudin family plays an important role in tight junction formation in the BBB, and the integrity of tight junctions was attenuated in an in vitro BBB model [29–36]. Therefore, we compared claudin protein profiles in vitro and in vivo (Fig. 7C). Five claudin proteins (CLDN1/Cldn1, CLDN5/Cldn5, CLDN7/Cldn7, CLDN11/Cldn11, and CLDN12/Cldn12) were abundantly detected in the present proteomic study, and the total claudin family expression levels were higher in BMVs in vivo (Fig. 7C). Additionally, the percentage of each claudin subtype in the total claudin family was compared between samples (Fig. 7D). Claudin-5 expression was the highest in BMVs, followed by primary cells and cell lines. Claudin-11 was highly expressed in all cell lines except MBEC4. The major claudin subtype in MBEC4 cells is claudin-12. Thus, the expression of the claudin subtype varies between BMVs and cultured BMECs, as well as among cell lines.

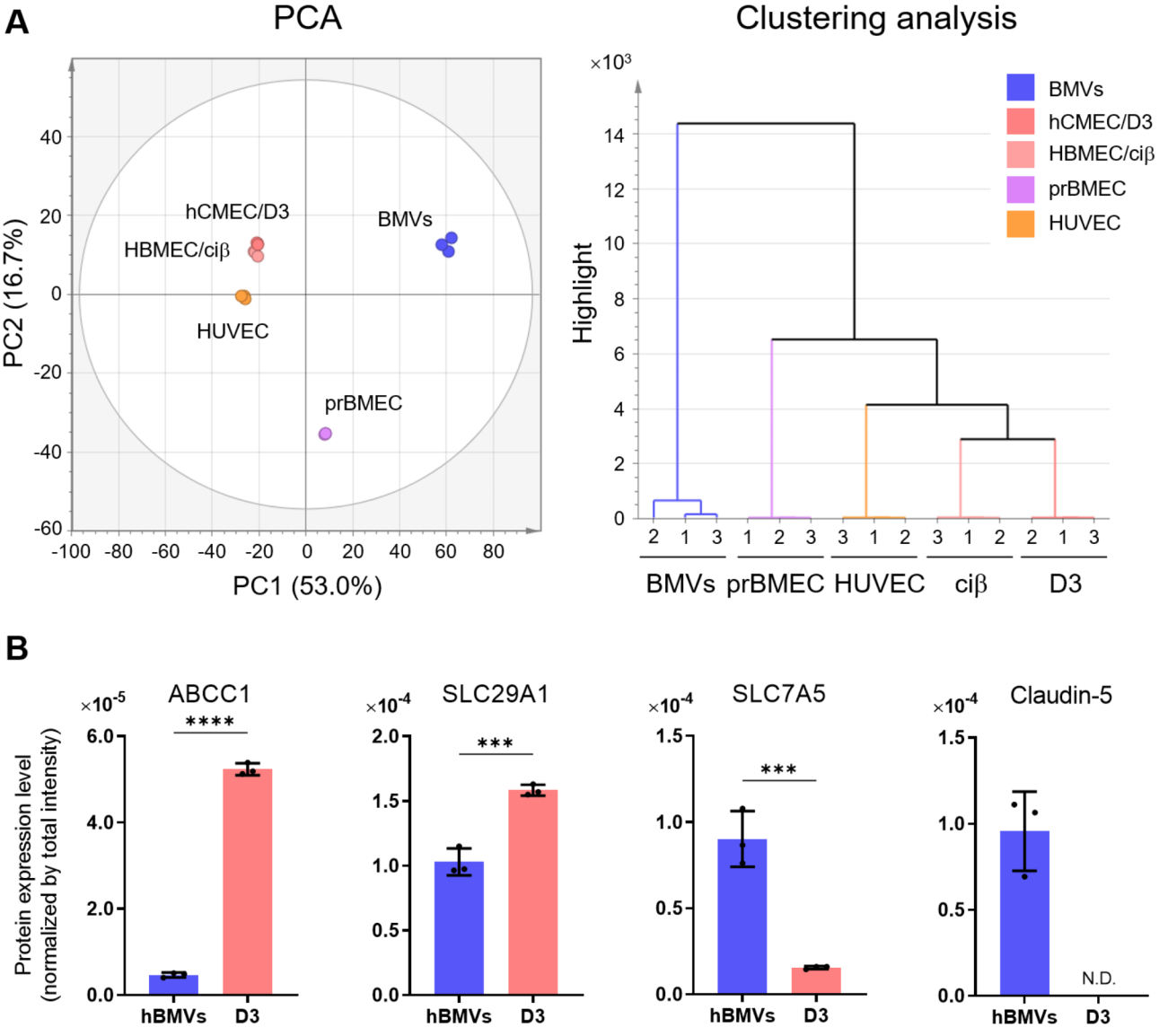

Fig. 6 Comparison of proteome profiles of human BMVs, cultured BMECs, and HUVECs. **A** PCA and clustering analysis of human BMV-enriched proteins in human BMV fractions and cultured brain microvascular endothelial cells (BMECs) ($n = 3$). **B** Protein expression levels of ABCC1, SLC29A1, SLC7A5, and claudin-5 in human BMV fractions and hCMEC/D3 cells. Each bar represents the mean ± SD ($n = 3$) and dots indicate the individual data. Statistical analyses were performed using a two-tailed Student's t-test. ***$p < 0.001$ and ****$p < 0.0001$

Discussion

The present study provides a deep proteomic profile of BMVs isolated from human, monkey, and mouse brain, as well as the profile of cultured BBB model cells. The profile obtained using DIA proteomics contained information on 7,000–8,000 proteins. Our previous study identified 1,527 proteins from mouse BMVs using DIA proteomics, but with older instruments and data analysis software than used in the present study [18]. Among the 1,527 proteins previously identified, 1,447 (94.8%) were also detected in the present study. Furthermore, we identified 6,788 proteins in mouse BMVs. A previous study identified 5,781 proteins from hCMEC/D3 using quantitative proteomics with data-dependent acquisition using different data analysis software [37]. Among the identified proteins, 5,195 (89.9%) were quantified using proteomic analysis, while the present study additionally detected 3,496 proteins. These results suggest the high depth and reproducibility of the proteome data.

In the present study, BMVs were isolated from frozen brains, and the enrichment of BMVs in the isolated fraction was assessed through the enrichment of BMEC markers and the removal of a neuronal marker (PSD95/Psd95). Claudin-5 enrichment and PSD95 removal were similar in the BMV fractions isolated from all species using western blotting (Fig. 1B). However, the proteome

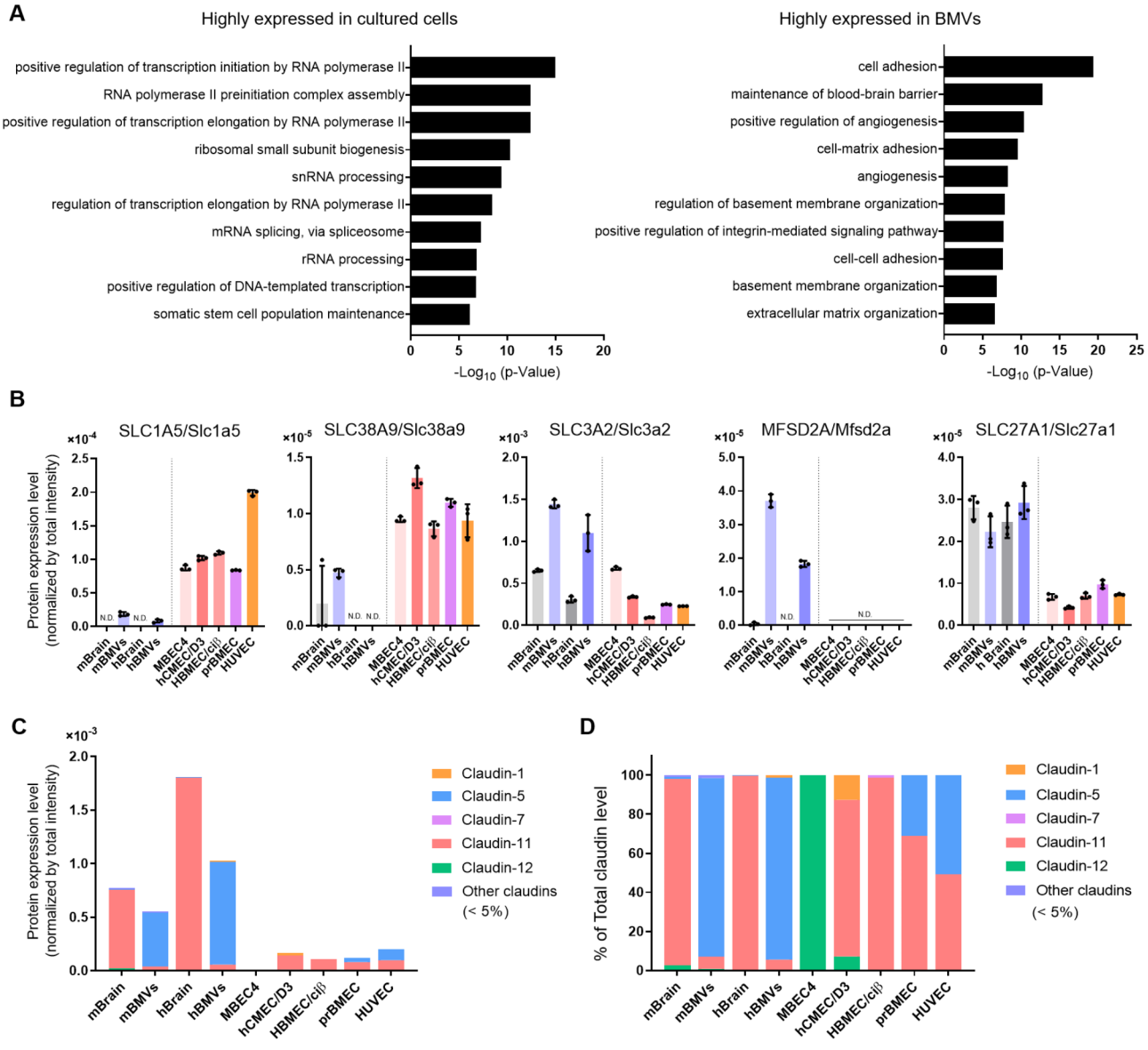

Fig. 7 Differences in protein expression between BMVs and cultured BMECs. **A** GO enrichment analysis of proteins highly expressed in either cultured human BMECs or BMVs. The top 10 enriched GO terms of biological process are shown. **B** Protein expression levels of SLC1A5/Slc1a5, SLC38A9/Slc38a9, SLC3A2/Slc3a2, MFSD2A/Mfsd2a, and SLC27A1/Slc27a1 in mouse, human BMVs, and cultured cells. Each bar represents the mean ± SD ($n = 3$), and dots indicate the individual data. **C** Expression levels of the claudin family members in mouse and human BMVs and cultured cells. Other claudin include CLDN/Cldn10, CLDN/Cldn14, CLDN/Cldn15, and CLDN/Cldn23. **D** Relative protein expression percentages of claudins in mouse and human samples

data comparison in Fig. 4B shows a relatively lower enrichment of BMEC markers in humans than in mice and monkeys. Given the prolonged postmortem intervals (PMI) and blood contamination affect the proteome [38, 39], it is possible that a longer PMI in human specimens (2.5–4 h) affected the enrichment of BMVs in our samples compared with mice and monkeys. However, the difference in PMI in human specimens was not large enough to influence species difference analysis because the three proteome datasets of human BMVs formed one group in the PCA and clustering analysis (Fig. 4C). Additionally, blood removal through perfusion was performed prior to brain dissection in mice only. Therefore, these differences in brain conditions must be considered when interpreting the present proteome dataset. To evaluate the effect of blood removal, PCA and clustering analysis were performed with the proteome data removing abundant blood proteins and keratins (Fig. S3). The results were similar to those without removal (Fig. 4C), suggesting that the impact of blood removal is not significant for the species difference profiles of BMV-enriched proteins.

The distribution of PCA and clustering analysis of BMV-enriched proteins was more similar in monkeys and humans than in mice (Fig. 4C). In a comparison of

transport-related protein expression between humans and monkeys or mice using targeted proteomics, a higher correlation was observed between humans and monkeys than between humans and mice [10]. In the evolutionary phylogenetic tree, humans are more similar to monkeys than to mice [40], indicating that the protein expression profiles between species reproduce the evolutionary phylogenetic tree.

ABCB1/Abcb1a expression levels in BMVs were higher in mice than in primates, while ABCG2/Abcg2 expression was higher in monkeys than in humans or mice (Fig. 5A). Targeted proteomics has reported similar results [10]. These results suggested that the distribution of ABCB1/Abcb1a and ABCG2/Abcg2 substrates in the brain varied among mice, monkeys, and humans. Previous positron emission tomography imaging has shown that brain concentrations of erlotinib, a substrate of ABCB1/Abcb1a and ABCG2/Abcg2, are significantly increased by the inhibition of ABCB1/Abcb1a and ABCG2/Abcg2 with elacridar in mice and monkeys but were not significantly increased in humans [41, 42]. These positron emission tomography results of species difference suggested that ABCB1/Abcb1a and ABCG2/Abcg2 were mainly involved in the BBB efflux of erlotinib in mice and monkeys, respectively. Furthermore, the contribution of ABCB1/Abcb1a and ABCG2/Abcg2 to erlotinib efflux through the BBB is relatively low in humans compared with that in mice and monkeys.

Differences in the expression profiles of the organic anion transporters were observed in the BMVs of all three species (Fig. 5C). SLCOs are sodium-independent, transmembrane organic anion transporters. Human and mouse orthologs do not have one-to-one relationships; in SLCO1A, there is SLCO1A2 in humans and Slco1a1, Slco1a4, Slco1a5, and Slco1a6 in mice. In SLCO1B, SLCO1B1 and SLCO1B3 are present in humans and Slco1b2 in mice [43]. Using cell type-specific RNA-seq and immunohistochemistry, Slco1a4, Slco1c1, and SLCO2B1 have been reported to be expressed and localized in BMVs [44–47]. Furthermore, all SLCO transporters detected in the present proteomic analysis, including Slco1a4, Slco1c1, and SLCO2B1, were enriched in BMV fractions compared with brain lysates, suggesting their selective localization in BMVs. Similar to the present results, previous studies have shown species differences in SLCO1A2/Slco1a2 and SLCO1C1/Slco1c1 between humans and mice and in SLCO1A2/Slco1a2 between humans and monkeys [8, 46, 48]. Therefore, the species differences in the SLCO expression profiles in the present dataset were considered to reflect those in BMVs. The SLCO family is responsible for the transport of various drugs, and SLCO1A and SLCO2B transport statins and dopamine receptor agonists [49, 50]. Additionally, SLCO1C1/Slco1c1 transports thyroid hormones [51]. Therefore, the distribution of substrate drugs and thyroid hormones may be affected by differences in the expression profiles of SLCO transporters.

Slc22a6 and Slc22a8 were highly expressed in mouse BMVs, whereas those with low expression levels were not detected in human or monkey BMVs (Fig. 5A and D). Slc22a8 is localized in rat BMVs and is involved in the brain-to-blood efflux transport of drugs and endogenous substrates such as 6-mercaptopurine, 6-thioguanine, and homovanillic acid [52, 53]. In the kidney, SLC22A6/Slc22a6 and SLC22A8/Slc22a8 are localized in the proximal renal tubular epithelial cells and are cooperatively involved in renal excretion by overlapping substrates [54]. Therefore, Slc22a6 and Slc22a8 may play a cooperative role in transport across the rodent BBB. In humans, plasma HVA concentration of homovanillic acid is a diagnostic marker of central dopaminergic activity [55]. The brain distribution of 6-mercaptopurine and 6-thioguanine is limited in humans [56, 57]. However, SLC22A6 and SLC22A8 were not detected in human and monkey BMV fractions in previous and current studies (Fig. 5A and D) [8]. Therefore, alternative transporters are expected to be involved in the BBB transport of these compounds in humans and monkeys. A recent study by Kurosawa et al. demonstrated that SLC43A3 mediates 6-mercaptopurine production in BMECs differentiated from human induced pluripotent stem cells [58]. The present study demonstrated primate-specific expression of SLC43A3 in BMV fractions and cultured BMECs (Figs. 5E and F). Therefore, SLC43A3 is a candidate transporter for the transport of 6-mercaptopurine and 6-thioguanine across the human BBB.

We also obtained the proteome profiles of the cultured BMECs and HUVECs. Compared with immortalized human BMECs, primary cultured human BMECs showed a proteomic profile similar to that of human BMVs (Fig. 6A). Furthermore, the proteome profiles of the two immortalized human BMECs were more similar to those of HUVECs than to those of the primary cultured BMECs. It has been reported that the expression levels of several claudin proteins and occludin are lower in immortalized cells than in primary cultured BMECs and that BBB barrier function is also reduced in immortalized cells [13, 59]. Additionally, the expression levels of genes involved in angiogenesis, such as TIE-2/Tie-2, VEGF/Vegf, and Angiopoietin-2, are similar in immortalized BMECs and HUVECs; however, those in primary cultured BMECs are different from those in HUVECs [60, 61]. These results suggest that primary cultured BMECs retain the protein expression of BMVs, whereas immortalized BMECs have impaired BBB-selective protein expression and become closer to peripheral vascular endothelial cells.

Comparison of amino acid transporter expression in vivo and in vitro revealed higher expression levels of SLC7A5/Slc7a5 and SLC3A2/Slc3a2 in vivo and SLC1A5/Slc1a5 and SLC38A9/Slc38a9 in vitro (Figs. 6B and 7B). Cancer cells require large amounts of glutamine to produce energy for growth [62], and the SLC7A5/SLC3A2 dimer and SLC1A5 transport glutamine into cells [63]. Additionally, SLC7A5 and SLC38A9 on the lysosomal membrane activate mTORC1 and cell signaling to transmit amino acid deprivation [62, 64]. Thus, cells *in vitro* may have increased expression of these transporters because they supply intracellular glutamine, similar to cancer cells. In contrast, SLC7A5 showed a low expression in vitro (Fig. 6B). Hypoxic and nutritional conditions in cells affect the expression level of SLC7A5 [65–67]. Therefore, SLC7A5 expression may decrease in vitro because of the differences between in vivo and culture environments.

MFSD2A/Mfsd2a and SLC27A1/Slc27a1, which are involved in DHA transport, were highly expressed in vivo (Fig. 7B). DHA is required in the brain and has injurious effects on tumor cells [68–70]. Therefore, cells in vitro are in a state similar to that of tumor cells and may have reduced the expression of DHA transporters to survive. Furthermore, the lack of MFSD2A/Mfsd2a expression in cultured BMECs indicated the necessity of identifying BMEC lines expressing MFSD2A/Mfsd2a for the molecular analysis of BBB DHA transport.

In immortalized BMECs, the expression of genes that form tight junctions, such as claudin-5, occludin, and JAM2, is lower than in vivo, resulting in a weak barrier function [71, 72]. When comparing the expression profiles of the claudin family, claudin-5 was mainly expressed in BMVs in vivo, whereas claudin-11 was mainly expressed in cultured human BMECS, including primary cultured BMECs (Fig. 7D). MBEC4 mainly expresses claudin-12 and exhibits different claudin expression profiles in human BMECs. In mice, claudin-12 knockout did not affect BBB integrity [73]. The expression level of claudin-12 in MBEC4 cells was comparable to that in mouse BMVs (Fig. 7C). These results suggest that tight junctions are weak in MBEC4 cells, with low expression levels of claudin proteins other than claudin-12. Blood flow-induced shear stress increases the expression of the adhesion-binding proteins ZO-1 and claudin-5 [74]. Additionally, claudin-5 is downregulated by VEGF, histamine, and TNFα [75, 76]. In contrast, claudin-11 is upregulated by GATA, NF-YA, and CREB [77]. In the present proteome profile, the expression level of NF-YA was 1.7- to 3.2-fold higher in the cultured BMECs than in the BMV fraction (Table S5). The same expression trends of claudins as those of proteins were observed at the mRNA level (Table S6), indicating that the expression of claudin family members was repressed at the transcriptional level.

Conclusions

Comprehensive proteomic analysis identified species differences in transport-related proteins, including SLC43A3/Slc43a3, SLC22A6/Slc22a6, and SLCO transporters, in mouse, monkey, and human BMVs. in vivo–in vitro comparisons revealed differences in the expression levels of transporters involved in the transport of amino acids and DHA, as well as in the expression pattern of claudin proteins. This study provides an informative dataset for protein expression in the BBB. Furthermore, these findings may provide a comprehensive understanding of the BBB proteome across species and between in vivo and in vitro conditions, which is essential for interpreting BBB function and drug distribution in the brain.

Abbreviations

BBB	Blood-brain barrier
BMVs	Brain microvessels
BMECs	Brain microvascular endothelial cells
ABC transporter	ATP-binding cassette transporter
SLC transporter	Solute carrier transporter
QTAP	Quantitative targeted absolute proteomics
DIA	Data-independent acquisition
PTS	Phase transfer surfactant
GO	Gene ontology
TPM	Transcripts per million
PCA	Principal component analysis
SLCO Transporter	Solute carrier organic anion transporter
DHA	Docosahexaenoic acid
PMI	Postmortem interval

Supplementary Information

The online version contains supplementary material available at https://doi.org/10.1186/s12987-025-00650-z.

Supplementary Material 1: Figure S1. Distribution of normalized protein and gene intensities. Figure S2. Proteomic and RNA-seq analyses of primary cultured human BMECs and HUVECs. Figure S3. PCA and clustering analysis of BMV-enriched protein profile, excluding abundant blood proteins and keratins.

Supplementary Material 2: Table S1. Sample information for monkey and human cerebral cortex. Table S2. Normalized protein intensities in human samples. Table S3. Normalized protein intensities in mouse samples. Table S4. Normalized protein intensities in monkey samples. Table S5. Expression levels of orthologous protein in mouse, monkey, and human samples. Table S6. Expression levels of genes in mouse and human in vitro samples. Table S7. Expression levels of transport-related proteins that are more abundant in humans than in mice. Table S8. Expression levels of transport-related proteins that are more abundant in mice than in humans. Table S9. Expression levels of transport-related proteins that are more abundant in humans than in monkeys. Table S10. Expression levels of transport-related proteins that are more abundant in monkeys than in humans. Table S11. Enrichment ratio of SLCO family in the BMV fraction to brain lysate. Table S12. Expression levels of BMV-enrichment proteins with variable expression in vivo and in vitro.

Acknowledgements

Not applicable.

Author contributions
Kumabe H, Masuda T, Ito S, Furihata T, Toda A, Mogi M, Araki N, and Ohtsuki S contributed to the study design and manuscript revision. Furihata T, Toda A, and Mogi M contributed to the collection of the biological materials. Masuda T and Araki N contributed to the proteomic analysis. Kumabe H conducted the experiments and performed data analysis. Kumabe H and Ohtsuki S wrote the manuscript. All authors provided their final approval for the submitted manuscript.

Funding
This study was supported in part by JPSP KAKENHI (24K02195 and 23H04937) and AMED BINDS (24ama121018).

Data availability
Raw data files for proteomic analysis have been deposited in jPOST (http://jpostdb.org; jPOST ID: JPST003553/PXD06008), and proteome data is provided within the supplementary information files.

Declarations

Ethics approval and consent to participate
Human brain samples were obtained from ProteoGenex following official protocols and approved by the appropriate Institutional Review Board/Independent Ethics Committee, which adhered to the current Federal Regulations, the International Council for Harmonization of Technical Requirements for Pharmaceuticals for Human Use, Health Insurance Portability and Accountability Act of 1996, and Guidelines for Good Clinical Practice for the protection of human subjects.

Consent for publication
Not applicable.

Competing interests
The authors declare no competing interests.

Author details
[1]Department of Pharmaceutical Microbiology, Graduate School of Pharmaceutical Sciences, Kumamoto University, Kumamoto 862-0973, Japan
[2]Department of Pharmaceutical Microbiology, Faculty of Life Sciences, Kumamoto University, Kumamoto 862-0973, Japan
[3]Institute for Advanced Biosciences, Keio University, Tsuruoka 997-0017, Japan
[4]Laboratory of Advanced Drug Development Sciences, School of Pharmacy, Tokyo University of Pharmacy and Life Sciences, Tokyo 192-0392, Japan
[5]Drug Safety Research Laboratories, Shin Nippon Biomedical Laboratories, Ltd, Miyanoura, Kagoshima 891-1394, Japan
[6]Department of Tumor Genetics and Biology, Faculty of Life Sciences, Kumamoto University, Kumamoto 860-8556, Japan

Received: 22 January 2025 / Accepted: 4 April 2025
Published online: 30 May 2025

References

1. Abbott NJ, Rönnbäck L, Hansson E. Astrocyte-endothelial interactions at the blood-brain barrier. Nat Rev Neurosci. 2006;7(1):41–53.
2. Greene C, Campbell M. Tight junction modulation of the blood brain barrier: CNS delivery of small molecules. Tissue Barriers. 2016;4(1):e1138017.
3. Abbott NJ, Patabendige AA, Dolman DE, Yusof SR, Begley DJ. Structure and function of the blood-brain barrier. Neurobiol Dis. 2010;37(1):13–25.
4. Campos-Bedolla P, Walter FR, Veszelka S, Deli MA. Role of the blood-brain barrier in the nutrition of the central nervous system. Arch Med Res. 2014;45(8):610–38.
5. Puris E, Fricker G, Gynther M. Targeting transporters for drug delivery to the brain: can we do better? Pharm Res. 2022;39(7):1415–55.
6. Miller DS. Regulation of ABC transporters at the blood-brain barrier. Clin Pharmacol Ther. 2015;97(4):395–403.
7. Parvez MM, Sadighi A, Ahn Y, Keller SF, Enoru JO. Uptake transporters at the blood-brain barrier and their role in brain drug disposition. Pharmaceutics. 2023;15(10):2473.
8. Uchida Y, Ohtsuki S, Katsukura Y, Ikeda C, Suzuki T, Kamiie J, et al. Quantitative targeted absolute proteomics of human blood-brain barrier transporters and receptors. J Neurochem. 2011;117(2):333–45.
9. Hoshi Y, Uchida Y, Tachikawa M, Inoue T, Ohtsuki S, Terasaki T. Quantitative atlas of blood-brain barrier transporters, receptors, and tight junction proteins in rats and common marmoset. J Pharm Sci. 2013;102(9):3343–55.
10. Uchida Y. Quantitative proteomics-based blood-brain barrier study. Biol Pharm Bull. 2021;44(4):465–73.
11. Syvänen S, Lindhe O, Palner M, Kornum BR, Rahman O, Långström B, et al. Species differences in blood-brain barrier transport of three positron emission tomography radioligands with emphasis on P-glycoprotein transport. Drug Metab Dispos. 2009;37(3):635–43.
12. Ohtsuki S, Ikeda C, Uchida Y, Sakamoto Y, Miller F, Glacial F, et al. Quantitative targeted absolute proteomic analysis of transporters, receptors and junction proteins for validation of human cerebral microvascular endothelial cell line hCMEC/D3 as a human blood-brain barrier model. Mol Pharm. 2013;10(1):289–96.
13. Berndt P, Winkler L, Cording J, Breitkreuz-Korff O, Rex A, Dithmer S, et al. Tight junction proteins at the blood-brain barrier: Far more than claudin-5. Cell Mol Life Sci. 2019;76(10):1987–2002.
14. Ludwig C, Gillet L, Rosenberger G, Amon S, Collins BC, Aebersold R. Data-independent acquisition-based SWATH-MS for quantitative proteomics: a tutorial. Mol Syst Biol. 2018;14(8):e8126.
15. Demichev V, Messner CB, Vernardis SI, Lilley KS, Ralser M. DIA-NN: neural networks and interference correction enable deep proteome coverage in high throughput. Nat Methods. 2020;17(1):41–4.
16. Gu K, Kumabe H, Yamamoto T, Tashiro N, Masuda T, Ito S, et al. Improving proteomic identification using narrow isolation windows with Zeno SWATH data-independent acquisition. J Proteome Res. 2024;23(8):3484–95.
17. Kawashima Y, Nagai H, Konno R, Ishikawa M, Nakajima D, Sato H, et al. Single-shot 10K proteome approach: over 10,000 protein identifications by data-independent acquisition-based single-shot proteomics with ion mobility spectrometry. J Proteome Res. 2022;21(6):1418–27.
18. Ogata S, Ito S, Masuda T, Ohtsuki S. Efficient isolation of brain capillary from a single frozen mouse brain for protein expression analysis. J Cereb Blood Flow Metab. 2021;41(5):1026–38.
19. Ogata S, Ito S, Masuda T, Ohtsuki S. Isolation method of brain microvessels from small frozen human brain tissue for blood-brain barrier protein expression analysis. Fluids Barriers CNS. 2024;21(1):106.
20. Masuda T, Tomita M, Ishihama Y. Phase transfer surfactant-aided trypsin digestion for membrane proteome analysis. J Proteome Res. 2008;7(2):731–40.
21. Tatsuta T, Naito M, Oh-hara T, Sugawara I, Tsuruo T. Functional involvement of P-glycoprotein in blood-brain barrier. J Biol Chem. 1992;267(28):20383–91.
22. Weksler BB, Subileau EA, Perriere N, Charneau P, Holloway K, Leveque M, et al. Blood-brain barrier-specific properties of a human adult brain endothelial cell line. FASEB J. 2005;19(13):1872–4.
23. Kamiichi A, Furihata T, Kishida S, Ohta Y, Saito K, Kawamatsu S, et al. Establishment of a new conditionally immortalized cell line from human brain microvascular endothelial cells: a promising tool for human blood-brain barrier studies. Brain Res. 2012;1488:113–22.
24. Kamiichi A, Furihata T, Kishida S, Ohta Y, Saito K, Kawamatsu S, et al. Establishment of a new conditionally immortalized cell line from human brain microvascular endothelial cells: a promising tool for human blood-brain barrier studies. Brain Res. 2012;1488:113–22.
25. Masuda T, Hoshiyama T, Uemura T, Hirayama-Kurogi M, Ogata S, Furukawa A, et al. Large-scale quantitative comparison of plasma transmembrane proteins between two human blood-brain barrier model cell lines, hCMEC/D3 and HBMEC/ciβ. Mol Pharm. 2019;16(5):2162–71.
26. Kawashima Y, Watanabe E, Umeyama T, Nakajima D, Hattori M, Honda K, et al. Optimization of data-independent acquisition mass spectrometry for deep and highly sensitive proteomic analysis. Int J Mol Sci. 2019;20(23):5932.
27. Hamada Y, Masuda T, Ito S, Ohtsuki S. Regulatory role of eIF2αK4 in amino acid transporter expression in mouse brain capillary endothelial cells. Pharm Res. 2024;41(11):2213–23.
28. Demichev V, Messner CB, Vernardis SI, Lilley KS, Ralser M. DIA-NN: neural networks and interference correction enable deep proteome coverage in high throughput. Nat Methods. 2020;17(1):41–4.

29. Nagano H, Ito S, Masuda T, Ohtsuki S. Effect of insulin receptor-knockdown on the expression levels of blood-brain barrier functional proteins in human brain microvascular endothelial cells. Pharm Res. 2022;39(7):1561–74.
30. Varki A, Altheide TK. Comparing the human and chimpanzee genomes: searching for needles in a haystack. Genome Res. 2005;15(12):1746–58.
31. Ohtsuki S, Hirayama M, Ito S, Uchida Y, Tachikawa M, Terasaki T. Quantitative targeted proteomics for understanding the blood-brain barrier: towards pharmacoproteomics. Expert Rev Proteomics. 2014;11(3):303–13.
32. Quan L, Ohgaki R, Hara S, Okuda S, Wei L, Okanishi H, et al. Amino acid transporter LAT1 in tumor-associated vascular endothelium promotes angiogenesis by regulating cell proliferation and VEGF-A-dependent mTORC1 activation. J Exp Clin Cancer Res. 2020;39(1):266.
33. Dolgodilina E, Imobersteg S, Laczko E, Welt T, Verrey F, Makrides V. Brain interstitial fluid glutamine homeostasis is controlled by blood-brain barrier SLC7A5/LAT1 amino acid transporter. J Cereb Blood Flow Metab. 2016;36(11):1929–41.
34. Cardoso FL, Brites D, Brito MA. Looking at the blood-brain barrier: molecular anatomy and possible investigation approaches. Brain Res Rev. 2010;64(2):328–63.
35. Angelow S, Ahlstrom R, Yu AS. Biology of claudins. Am J Physiol Ren Physiol. 2008;295(4):F867–76.
36. Shah B, Dong X. Current status of in vitro models of the blood-brain barrier. Curr Drug Deliv. 2022;19(10):1034–46.
37. Choublier N, Taghi M, Menet MC, Le Gall M, Bruce J, Chafey P, et al. Exposure of human cerebral microvascular endothelial cells hCMEC/D3 to laminar shear stress induces vascular protective responses. Fluids Barriers CNS. 2022;19(1):41.
38. Crecelius A, Götz A, Arzberger T, Fröhlich T, Arnold GJ, Ferrer I, et al. Assessing quantitative post-mortem changes in the Gray matter of the human frontal cortex proteome by 2-D DIGE. Proteomics. 2008;8(6):1276–91.
39. Aasebø E, Opsahl JA, Bjørlykke Y, Myhr KM, Kroksveen AC, Berven FS. Effects of blood contamination and the rostro-caudal gradient on the human cerebrospinal fluid proteome. PLoS ONE. 2014;9(3):e90429.
40. Pozzi L, Hodgson JA, Burrell AS, Sterner KN, Raaum RL, Disotell TR. Primate phylogenetic relationships and divergence dates inferred from complete mitochondrial genomes. Mol Phylogenet Evol. 2014;75:165–83.
41. Tournier N, Goutal S, Auvity S, Traxl A, Mairinger S, Wanek T, et al. Strategies to inhibit ABCB1- and ABCG2-mediated efflux transport of erlotinib at the blood-brain barrier: a PET study on nonhuman primates. J Nucl Med. 2017;58(1):117–22.
42. Verheijen RB, Yaqub M, Sawicki E, van Tellingen O, Lammertsma AA, Nuijen B, et al. Molecular imaging of ABCB1 and ABCG2 Inhibition at the human blood-brain barrier using Elacridar and (11)C-erlotinib PET. J Nucl Med. 2018;59(6):973–9.
43. Iusuf D, van de Steeg E, Schinkel AH. Functions of OATP1A and 1B transporters in vivo: insights from mouse models. Trends Pharmacol Sci. 2012;33(2):100–8.
44. Zhang Y, Chen K, Sloan SA, Bennett ML, Scholze AR, O'Keeffe S, et al. An RNA-sequencing transcriptome and splicing database of glia, neurons, and vascular cells of the cerebral cortex. J Neurosci. 2014;34(36):11929–47.
45. Ose A, Kusuhara H, Endo C, Tohyama K, Miyajima M, Kitamura S, et al. Functional characterization of mouse organic anion transporting peptide 1a4 in the uptake and efflux of drugs across the blood-brain barrier. Drug Metab Dispos. 2010;38(1):168–76.
46. Roberts LM, Woodford K, Zhou M, Black DS, Haggerty JE, Tate EH, et al. Expression of the thyroid hormone transporters monocarboxylate transporter-8 (SLC16A2) and organic ion transporter-14 (SLCO1C1) at the blood-brain barrier. Endocrinology. 2008;149(12):6251–61.
47. Gao B, Vavricka SR, Meier PJ, Stieger B. Differential cellular expression of organic anion transporting peptides OATP1A2 and OATP2B1 in the human retina and brain: implications for carrier-mediated transport of neuropeptides and neurosteriods in the CNS. Pflugers Arch. 2015;467(7):1481–93.
48. Ito K, Uchida Y, Ohtsuki S, Aizawa S, Kawakami H, Katsukura Y, et al. Quantitative membrane protein expression at the blood-brain barrier of adult and younger cynomolgus monkeys. J Pharm Sci. 2011;100(9):3939–50.
49. Kalliokoski A, Niemi M. Impact of OATP transporters on pharmacokinetics. Br J Pharmacol. 2009;158(3):693–705.
50. Schäfer AM, Meyer Zu Schwabedissen HE, Bien-Möller S, Hubeny A, Vogelgesang S, Oswald S, et al. OATP1A2 and OATP2B1 are interacting with Dopamine-Receptor agonists and antagonists. Mol Pharm. 2020;17(6):1987–95.
51. Sugiyama D, Kusuhara H, Taniguchi H, Ishikawa S, Nozaki Y, Aburatani H, et al. Functional characterization of rat brain-specific organic anion transporter (Oatp14) at the blood-brain barrier: high affinity transporter for thyroxine. J Biol Chem. 2003;278(44):43489–95.
52. Mori S, Ohtsuki S, Takanaga H, Kikkawa T, Kang YS, Terasaki T. Organic anion transporter 3 is involved in the brain-to-blood efflux transport of thiopurine nucleobase analogs. J Neurochem. 2004;90(4):931–41.
53. Mori S, Takanaga H, Ohtsuki S, Deguchi T, Kang YS, Hosoya K, et al. Rat organic anion transporter 3 (rOAT3) is responsible for brain-to-blood efflux of homovanillic acid at the abluminal membrane of brain capillary endothelial cells. J Cereb Blood Flow Metab. 2003;23(4):432–40.
54. Vallon V, Rieg T, Ahn SY, Wu W, Eraly SA, Nigam SK. Overlapping in vitro and in vivo specificities of the organic anion transporters OAT1 and OAT3 for loop and Thiazide diuretics. Am J Physiol Ren Physiol. 2008;294(4):F867–73.
55. Lambert GW, Eisenhofer G, Cox HS, Horne M, Kalff V, Kelly M, et al. Direct determination of homovanillic acid release from the human brain, an indicator of central dopaminergic activity. Life Sci. 1991;49(15):1061–72.
56. Zimm S, Ettinger LJ, Holcenberg JS, Kamen BA, Vietti TJ, Belasco J, et al. Phase I and clinical Pharmacological study of mercaptopurine administered as a prolonged intravenous infusion. Cancer Res. 1985;45(4):1869–73.
57. Adamson PC, Balis FM, Arndt CA, Holcenberg JS, Narang PK, Murphy RF, et al. Intrathecal 6-mercaptopurine: preclinical pharmacology, phase I/II trial, and Pharmacokinetic study. Cancer Res. 1991;51(22):6079–83.
58. Kurosawa T, Tega Y, Sako D, Mochizuki T, Yamaguchi T, Kawabata K, et al. Transport characteristics of 6-mercaptopurine in brain microvascular endothelial cells derived from human induced pluripotent stem cells. J Pharm Sci. 2021;110(10):3484–90.
59. Veszelka S, Tóth A, Walter FR, Tóth AE, Gróf I, Mészáros M, et al. Comparison of a rat primary cell-based blood-brain barrier model with epithelial and brain endothelial cell lines: gene expression and drug transport. Front Mol Neurosci. 2018;11:166.
60. Kallmann BA, Wagner S, Hummel V, Buttmann M, Bayas A, Tonn JC, et al. Characteristic gene expression profile of primary human cerebral endothelial cells. Faseb J. 2002;16(6):589–91.
61. van Beijnum JR, van der Linden E, Griffioen AW. Angiogenic profiling and comparison of immortalized endothelial cells for functional genomics. Exp Cell Res. 2008;314(2):264–72.
62. Scalise M, Pochini L, Galluccio M, Indiveri C. Glutamine transport. From energy supply to sensing and beyond. Biochim Biophys Acta. 2016;1857(8):1147–57.
63. Yanagida O, Kanai Y, Chairoungdua A, Kim DK, Segawa H, Nii T, et al. Human L-type amino acid transporter 1 (LAT1): characterization of function and expression in tumor cell lines. Biochim Biophys Acta. 2001;1514(2):291–302.
64. Wang S, Tsun ZY, Wolfson RL, Shen K, Wyant GA, Plovanich ME, et al. Metabolism. Lysosomal amino acid transporter SLC38A9 signals arginine sufficiency to mTORC1. Science. 2015;347(6218):188–94.
65. Boado RJ, Li JY, Tsukamoto H, Pardridge WM. Hypoxia induces de-stabilization of the LAT1 large neutral amino acid transporter mRNA in brain capillary endothelial cells. J Neurochem. 2003;85(4):1037–42.
66. Ozgür B, Helms HCC, Tornabene E, Brodin B. Hypoxia increases expression of selected blood-brain barrier transporters GLUT-1, P-gp, SLC7A5 and TFRC, while maintaining barrier integrity, in brain capillary endothelial monolayers. Fluids Barriers CNS. 2022;19(1):1.
67. Nachef M, Ali AK, Almutairi SM, Lee SH. Targeting SLC1A5 and SLC3A2/SLC7A5 as a potential strategy to strengthen anti-tumor immunity in the tumor microenvironment. Front Immunol. 2021;12:624324.
68. Connor WE. Importance of n-3 fatty acids in health and disease. Am J Clin Nutr. 2000;71(1 Suppl):s171–5.
69. Karmali RA, Marsh J, Fuchs C. Effect of omega-3 fatty acids on growth of a rat mammary tumor. J Natl Cancer Inst. 1984;73(2):457–61.
70. Gonzalez MJ, Schemmel RA, Dugan L Jr., Gray JI, Welsch CW. Dietary fish oil inhibits human breast carcinoma growth: a function of increased lipid peroxidation. Lipids. 1993;28(9):827–32.
71. Urich E, Lazic SE, Molnos J, Wells I, Freskgård PO. Transcriptional profiling of human brain endothelial cells reveals key properties crucial for predictive in vitro blood-brain barrier models. PLoS ONE. 2012;7(5):e38149.
72. Weksler B, Romero IA, Couraud PO. The hCMEC/D3 cell line as a model of the human blood brain barrier. Fluids Barriers CNS. 2013;10(1):16.
73. Castro Dias M, Coisne C, Baden P, Enzmann G, Garrett L, Becker L, et al. Claudin-12 is not required for blood-brain barrier tight junction function. Fluids Barriers CNS. 2019;16(1):30.
74. Molins B, Mora A, Romero-Vázquez S, Pascual-Méndez A, Rovira S, Figueras-Roca M, et al. Shear stress modulates inner blood retinal barrier phenotype. Exp Eye Res. 2019;187:107751.

75. Laakkonen JP, Lappalainen JP, Theelen TL, Toivanen PI, Nieminen T, Jauhiainen S, et al. Differential regulation of angiogenic cellular processes and claudin-5 by Histamine and VEGF via PI3K-signaling, transcription factor SNAI2 and interleukin-8. Angiogenesis. 2017;20(1):109–24.
76. Aslam M, Ahmad N, Srivastava R, Hemmer B. TNF-alpha induced NFκB signaling and p65 (RelA) overexpression repress Cldn5 promoter in mouse brain endothelial cells. Cytokine. 2012;57(2):269–75.
77. Lui WY, Wong EW, Guan Y, Lee WM. Dual transcriptional control of claudin-11 via an overlapping GATA/NF-Y motif: positive regulation through the interaction of GATA, NF-YA, and CREB and negative regulation through the interaction of Smad, HDAC1, and mSin3A. J Cell Physiol. 2007;211(3):638–48.

Publisher's note